buildings

MDPI

Article

Static Mechanical Properties of Aeolian Sand Improved with Silt Subjected to Varying Temperature and Pressure

Bojun Cui, Jian Xu *, Xianxian Shao, Dechao Xu and Bingqi Zhang

College of Water Conservancy and Hydropower Engineering, Gansu Agricultural University, Lanzhou 730070, China; cuibojun999@163.com (B.C.)
* Correspondence: xujian@gsau.edu.cn

Abstract: Delineating the mechanical characteristics of aeolian sand improved with silt under temperature action is of great significance for the construction and long-term operation of engineering materials in seasonal frozen areas. Against the backdrop of aeolian sand resource utilization in the western region, local obtainable wind turbine sand and silt were used as raw materials, and a series of triaxial compression tests were conducted on aeolian sand improved with silt through temperature-controlled triaxial testers. The experimental parameters were as follows: silt content of 0%, 5%, 10%, 15%, and 20%; confining pressures of 100 kPa, 200 kPa, and 300 kPa; and temperatures of room temperature, 0 °C, −5 °C, −10 °C, and −15 °C. The results of the experiment demonstrated that the interaction between silt dosage, confining pressure, and temperature effects significantly influenced the triaxial compression strength of aeolian sand improved with silt. As the dosage of silt increased from 0% to 15%, the peak strength of the samples rose by 7.72% to 18.03%. This maximum increase occurred at a silt dosage of 15%. With the increase in confining pressures, the stress–strain relationship curve for the sample exhibits strain softening characteristics. Under varying temperatures, the samples exhibited a consistent pattern of initial shrinkage followed by subsequent expansion. As temperatures decrease, cohesive forces exhibit a wavelike pattern in their variation, with an essentially constant internal friction angle. The research results can provide theoretical support for the selection of building materials in the northwest region, address the issue of regional material shortages, and improve the application of aeolian sand in seasonally frozen areas.

Keywords: improved aeolian sand; silt; optimal mixing ratio; temperature effect; triaxial compression test

Citation: Cui, B.; Xu, J.; Shao, X.; Xu, D.; Zhang, B. Static Mechanical Properties of Aeolian Sand Improved with Silt Subjected to Varying Temperature and Pressure. *Buildings* **2024**, *14*, 3801. https://doi.org/10.3390/buildings14123801

Academic Editor: Grzegorz Ludwik Golewski

Received: 27 October 2024
Revised: 18 November 2024
Accepted: 26 November 2024
Published: 28 November 2024

1. Introduction

In the northwest region of China, ample reserves of aeolian sand abound. If this material can be employed in construction projects, it not only caters to the vast demands for construction materials but also yields significant economic benefits and environmental gains. However, aeolian sand is beset by numerous defects such as loose structure [1], substandard gradation [2], limited cohesion or no cohesion [3], and low shear strength [4], which collectively result in poor engineering properties.

At present, various improvement methods are commonly employed to enhance the mechanical properties of aeolian sand. For instance, Huang et al. [5] employed cement modification for aeolian sand, finding that as the cement content increases, the unconfined compressive strength follows power function growth. Yang et al. [6] employed fiber- and silt-reinforced cement improved aeolian sand, finding that fiber and silt can significantly improve the strength and ductility of cement-stabilized aeolian sand. Ruan et al. [7,8] employed fiber cement improved sand for blast furnace slag, discovering that the blended use of fiber cement improved unconfined compressive strength of aeolian sand' by 12–46% compared to its single addition fiber. Wei et al. [9] employed fine angular gravel to improve aeolian sand, revealing that aeolian sand is a badly graded sand. Not only did the addition

of fine angular gravel enhance the particle gradation of aeolian sand, but it also improved the mechanical properties of aeolian sand.

On the other hand, the mechanical properties of engineering materials may exhibit significant variations under different temperature conditions. Hence, temperature effects are another crucial factor that cannot be overlooked when studying the mechanical characteristics of engineering materials. Jing et al. [10] found that the impact of high temperatures on the moisture content and pore water pressure in eolian sand subgrade decreased gradually, with a delay effect. Bao et al. [11] discovered that as the number of freeze–thaw cycles and salt content increased, the softening rate of aeolian sand strain significantly decreased. Under different numbers of freeze–thaw cycles, the initial rebound modulus of aeolian sand increased with confining pressures, increasing initially and then slowly increasing as the cycle number increased. Liu et al. [12] found that the stress–strain curves of cement aeolian sand improved with silt exhibited strain softening characteristics under normal temperatures; the elastic modulus, failure strength, cohesion force, and internal friction angle of aeolian sand were all increased upon the addition of cement silt.

As shown by the above analysis, in view of improving the aeolian sand, aeolian sand often employs the method of incorporating cement or fiber cement to enhance the performance of aeolian sand. Despite its remarkable improvement in mechanical performance, actual construction encounters high costs for cement, fibers, and transportation, as well as difficulties in construction. The northwestern region boasts abundant silt reserves. If harnessed appropriately, adopting silt to enhance the performance of aeolian sand would hold immense significance for local construction efforts.

From a temperature effect perspective, studies on the influence of mechanical properties of aeolian sand under different conditions have mainly focused on ambient, high-temperature, and freeze–thaw cycles. Research into the impact of varying temperatures on its static characteristics is still relatively limited. Consequently, the study of the thermomechanical properties of aeolian sand improved with silt under varying temperature conditions holds significant engineering application value.

In summary, based on current research and experimental results related to the improved aeolian sand modification plans and temperature effects, the economic viability of the modified materials has not been well addressed in practical engineering: in-depth studies on the effects of ambient and low temperatures on improved aeolian sand are still limited. Therefore, this study investigates the static characteristics of aeolian sand improved with silt under different temperature conditions through static triaxial compression experiments. The research results can provide theoretical support for the selection of building materials in the northwest region, address the issue of regional material shortages, and improve the application of aeolian sand in seasonally frozen areas.

2. Materials and Methods

2.1. Experimental Material

Both aeolian sand and silt were sourced from the Gulang County Huanghuatan Reservoir Field in Gansu Province. Aeolian sand is primarily composed of lithic rock, feldspar, and quartz, with a clay content ranging from 3.2% to 5.6%. Its natural density ranges from 1.48 to 1.56 g/cm^3, with a natural moisture content varying between 3.0% and 5.0%. The natural angle of repose lies between 28.5° and 29.2°; its cohesion ranges from 0.5 to 2.3 kPa. The main grain size distribution is within the range of 0.075 to 0.5 mm, with a single grain size, curve coefficient ranging from 0.83 to 0.92, and an unevenness coefficient ranging from 2.35 to 3.21 [13,14]. Aeolian sand is categorized as badly graded sand [15].

Silt has a natural density of 1.57 g/cm^3, an optimal moisture content of 10.92%, a specific gravity of 2.68, a liquid limit of 21.2%, and a plastic limit of 12.0%. Its plasticity index is 9.2, categorizing it as a low-liquid-limit silt [16].

To ensure that laboratory conditions are as close as possible to actual field conditions, the test aeolian sand and silt were only subjected to impurity removal and sieving through a 5 mm mesh.

2.2. Experimental Equipment

The MTS-810 triaxial material testing machine produced by American MTS Corporation was utilized for the triaxial compression test. Figure 1 depicts the concrete figure of the triaxial compression testing instrument., a three-axis material testing machine consisting of an MTS-285 hydraulic system, an MTS-810 material testing machine, a triaxial pressure chamber, a temperature-controlled recirculating refrigeration system, and a data automatic collection system. The maximum axial load capacity of the instrument is 100 kN, with pressure ranges of 0.3 to 20.0 MPa for confining pressures, a maximum axial displacement of ±85 mm, a frequency range of 0 to 50 Hz, and a temperature range from ambient to −30 °C. The measurement accuracy is as follows: a long-term accuracy of ±3% and a short-term accuracy of ±1% [17].

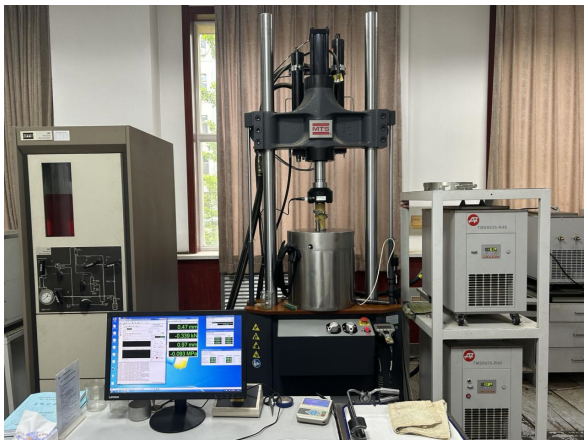

Figure 1. The MTS-810 triaxial material testing machine.

2.3. Methods of Experiment

2.3.1. Experiment Scheme Design

The test was conducted utilizing an MTS-810 triaxial material testing machine. A series of triaxial compression experiments were conducted based on GBT50123—2019 "Standard for geotechnical testing method" [18]. To compare stress–strain curves and shear strength indicators under different silt concentrations and confining pressures states for aeolian sand improved with silt, the experimental design considered silt concentrations (W_S = 0%, 5%, 10%, 15%, and 20%) and confining pressure conditions (σ_3 = 100, 200, and 300 kPa) for modified aeolian sand samples under a consolidated undrained triaxial test. In this way, an optimal silt concentration was sought under normal temperature conditions. Through this optimal concentration, consolidated undrained triaxial test were conducted at different temperatures (T = Rt, −5 °C, −10 °C, −15 °C, and −20 °C) to investigate the effect of temperature on the mechanical properties of aeolian sand improved with silt, with a view to assessing the feasibility of adopting aeolian sand improved with silt in engineering projects in the northwest region, thus providing reference for construction. In the loading process, the sample was subjected to a radial load at a rate of 1.25 mm/min until a deformation of 20% was achieved, while maintaining constant confining pressures. The experiment scheme is as shown in Table 1.

Table 1. The triaxial experiment scheme.

W_S/%	σ_3/kPa	K	T/°C	γ/(mm/min)
0, 5, 10, 15, 20 Optimal dosage	100, 200, 300	1.0	Rt 0, −5, −10, −15	1.25

2.3.2. The Method of Sample Preparation

In accordance with GBT50123—2019 "Standard for geotechnical testing method", the optimal water content and maximum dry density for different silt admixtures (W_S = 0%, 5%, 10%, 15%, and 20%) were obtained through compaction tests of aeolian sand modified with various percentages. The results are shown in Table 2. Taking into account the impact of differing moisture content on the tests, all soil samples were prepared using their optimal water content. The experiment was conducted under both room temperature conditions and low-temperature conditions, with slightly differing methods of sample preparation, as outlined in the following paragraphs.

Table 2. Eigenvalue of standard compaction tests.

W_S/%	ω_0/%	ρ_{dmax}/(g/cm^3)
0	14.8	1.73
5	13.8	1.71
10	11.9	1.75
15	11.5	1.80
20	11.9	1.83

Under room-temperature conditions, samples were determined by the silt dosage for various materials and their quality, with deionized water added to obtain the required moisture content. They were placed in sealed bags and left undisturbed for 24 h. Based on dry density calculations, the required wet soil mass was determined, and five layers of preparation of standard samples were conducted. The diameter and height of the samples were 61.8 mm and 125 mm.

Under low temperatures, samples were prepared using the same method as that used for the above ambient temperature samples. Then, the samples were placed in a −30 °C refrigerated cabinet for rapid freezing (ensuring even freezing), followed by 48 h of static storage in a controlled-temperature refrigerator before being left undisturbed for 24 h. During the trial, the samples were swiftly retrieved from the constant-temperature refrigerator and immediately placed into the triaxial pressure chamber under controlled temperature conditions. To mitigate temperature fluctuations during sampling, the samples were constant temperature for two hours in the controlled-temperature triaxial pressure chamber before the load testing began.

3. Results

3.1. The Stress–Strain Curves and Peak Strength Curves Under Varying Silt Ratios

Figures 2 and 3 display the stress–strain curves under different silt dosages compared to those under confining pressures.

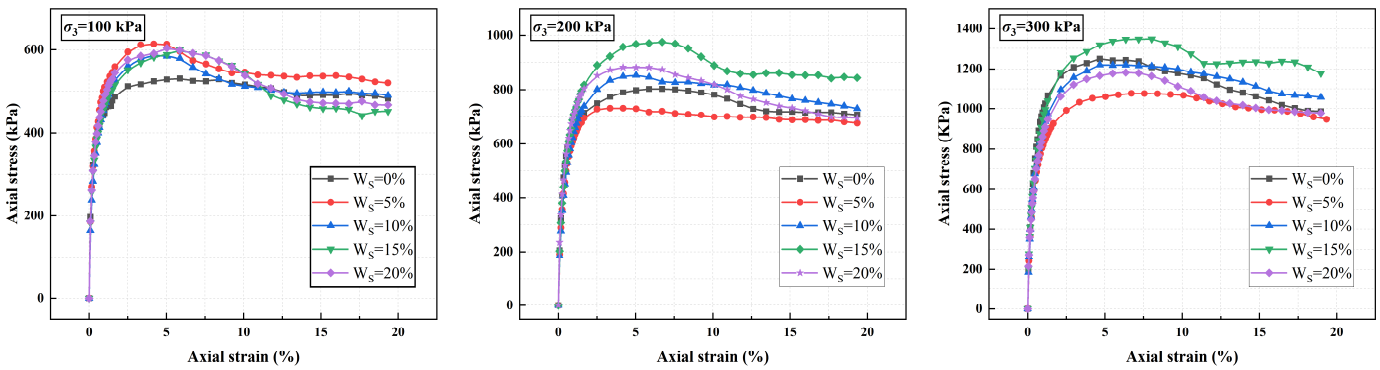

Figure 2. The stress–strain curve under different proportions of blending with clay aeolian sand improved with silt.

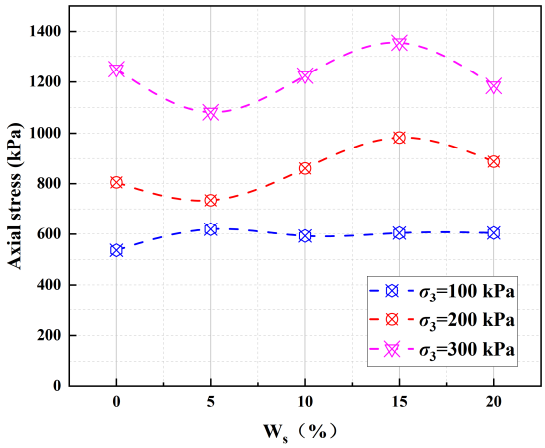

Figure 3. The peak strength curve of under different proportions of blending with clay aeolian sand improved with silt.

As depicted in Figure 1, the development trends in the primary stresses under different silt additions for the improved aeolian sand formulation exhibit a similar pattern, divided into three distinct phases:

(1) In the linear elastic stage, the stress increases rapidly with increasing strain, exhibiting linear elastic growth at smaller strains;
(2) In the elastic–plastic stage, as strain increases, the stress gradually transforms from linear to curvilinear, with the growth rate of normal stress (σ_1–σ_3) decreasing and eventually reaching a peak;
(3) In the shaping deformation stage, when the normal stress reaches its peak value, the normal stress (σ_1–σ_3) initially decreases gradually before stabilizing.

As depicted in Figure 2:

(1) At a confining pressure of σ_3 = 100 kPa, the peak strength of aeolian sand with no silt dosage is the smallest compared to other silt dosages. As W_S increases, the peak strength initially increases before stabilizing. At a silt dosage of W_S = 5%, the peak strength is at its maximum.
(2) At a confining pressure of σ_3 = 200 kPa, the minimum peak strength was exhibited by the improved aeolian sand with an addition of 5%, while the maximum peak strength was attained by the improved aeolian sand with an addition of 15%. As W_S increases, the peak intensity initially decreases before growing to a maximum value, after which it again decreases. Silt's dosage of W_S = 5% and 15% are critical values.
(3) At a confining pressure of σ_3 = 300 kPa, the peak strength follows the same law as that observed in trials with a confining pressure of σ_3 = 200 kPa.

As depicted in Table 3:

(1) At a confining pressure of σ_3 = 100 kPa, as the silt dosage increases, compared to aeolian sand without silt addition, the growth rate initially decreases before slightly increasing, with a more gradual change. The impact of silt dosage on the growth rate is not evident.
(2) At a confining pressure of σ_3 = 200 kPa, at a low silt dosage (5%), the growth rate was negative (−8.83%), but as the silt dosage increased to 10%, 15%, and 20%, the growth rate gradually turned positive, reaching a peak of 22.00% at a water content of 15%. A moderate addition of silt (15%) significantly enhanced the growth rate.
(3) At a confining pressure of σ_3 = 300 kPa, when the silt dosage was increased to 5%, the growth rate was negative (−13.48%). However, when the dosage rose to 10% and 15%, the growth rate reversed and reached 8.37%. However, when the silt dosage was increased to 20%, the growth rate decreased again to a negative value (−5.29%). Under the condition of a high confining pressure, the impact of the water content

on the growth rate is rather complex, with an optimal range of moisture content (approximately 10–15%).

Table 3. Compared to aeolian sand without the addition of silt, the percentage increase in peak strength.

σ_3/kPa	W_S/%	Growth Rate/%
100	5	15.53
	10	10.54
	15	12.66
	20	12.76
200	5	−8.83
	10	6.81
	15	22.00
	20	10.16
300	5	−13.48
	10	−2.06
	15	8.37
	20	−5.29

Summarily speaking, the stress–strain development law of aeolian sand with varying silt concentrations exhibits a similar trend: an initial rapid increase followed by a gradual decrease before approaching stability. This trend increases as the confining pressure increases. Under different confining pressure conditions, the improved aeolian sand exhibited the greatest peak strength when the addition rate was Ws = 15%. Consequently, silt dosage of W_S = 15% was deemed optimal for aeolian sand improved with silt.

3.2. Analysis of Stress–Strain Curve Under Different Temperature Conditions and Optimal Mixing Ratio

Based on the optimal mixing ratio Ws = 15% obtained from the previous experiment, experiments of triaxial compression under different temperature effects were conducted. The experimental results of aeolian sand improved with silt at different temperatures are shown in Figure 4.

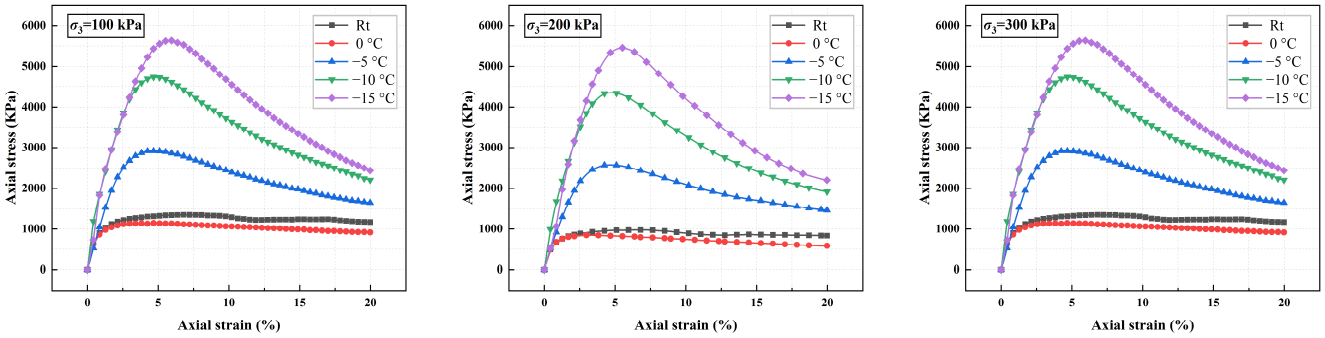

Figure 4. Stress–strain curve under different temperature conditions and optimal mixing ratio.

From Figure 4, it can be seen that the specimen is in a critical state at σ_3 = 100 kPa and temperature = 0 °C, with a 6.24% decrease in peak strength compared to room temperature conditions. As the temperature continues to decrease, the shear strength of aeolian sand significantly improved with silt increases, showing the property that the lower the temperature, the greater the shear strength. Peak strength at −5 °C is 75.24% higher than at room temperature; at −10 °C, it is 85.00% higher; and at −15 °C, it is 88.35% higher than at room temperature. Under other confining pressure conditions, the stress–strain law is roughly the same as σ_3 = 100 kPa.

3.3. Stress–Strain Curves and Total Stress Paths Under Different Confining Pressure Conditions with Optimal Mixing Ratio

Figure 5 shows the stress–strain curves and total stress paths of improved aeolian sand under different temperatures with an optimal mixing ratio and different confining pressure conditions. As shown in Figure 5, the peak intensity is related to the size of confining pressures, with the peak intensity increasing with the increase in confining pressure; the stress–strain curve gradually transitions from a weak strain softening type to a strong strain softening type as the temperature decreases. Under the optimal mixing ratio conditions, the total stress paths of the modified aeolian sand tend to be a straight line at different temperatures. With different confining pressures, the slopes of the straight total stress paths are basically the same and tend to be parallel to each other. The dense points of the total stress paths always appear above and to the right of the straight line. This finding aligns with Mao et al.'s research results [19]. The lower the temperature, the denser the total stress paths are under different confining pressures.

3.4. Shear Strength

Aeolian sand improved with the silt shear strength index under different temperature conditions and an optimal blending ratio is shown in Table 4. The cohesion shows a pattern of initially increasing and then decreasing with the decrease in temperature, which may be due to the freezing of moisture as the temperature drops, enhancing cohesion between particles. However, as the temperature continues to decrease, the structure becomes brittle, leading to a decrease in cohesion [20]. The variation in the friction angle remains relatively stable between room temperature and −10 °C, but decreases significantly at −15 °C. At its core, this is largely due to an increase in ice crystals at lower freezing temperatures, which in turn leads to an increase in unfrozen water content during shearing. Consequently, a more prominent lubrication effect occurs, resulting in a decrease in the friction angle [21].

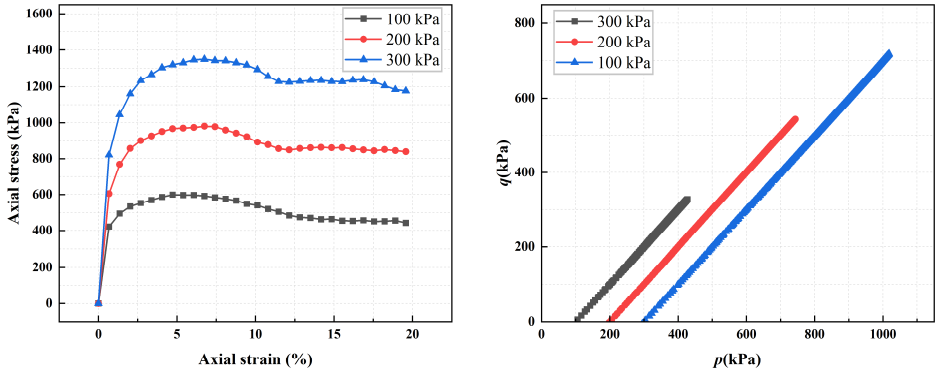

T = room temperature

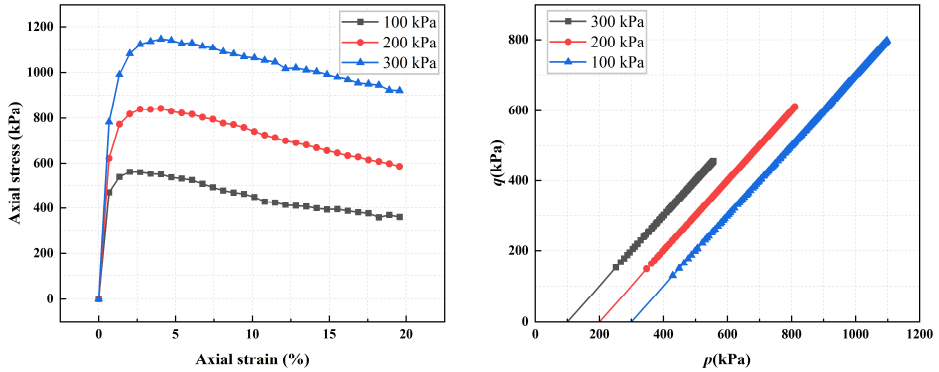

T = 0 °C

Figure 5. *Cont.*

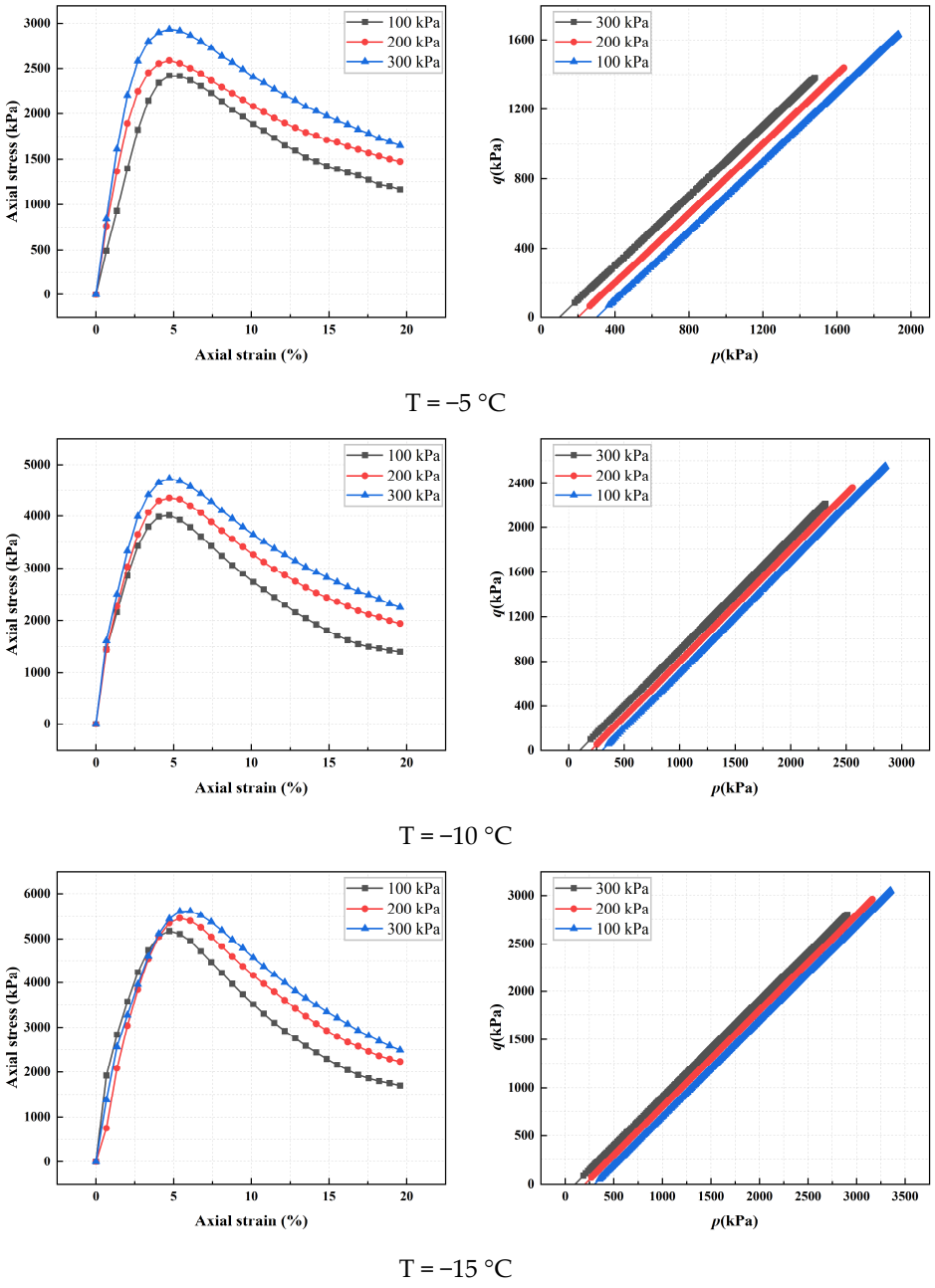

Figure 5. Stress–strain curves and total stress paths of improved aeolian sand under different temperatures with optimal mixing ratio and different confining pressure conditions.

Table 4. Aeolian sand improved with silt shear strength index under different temperature conditions and optimal blending ratio.

Shear Strength Parameters	Rt	0 °C	−5 °C	−10 °C	−15 °C
c/kPa	120	490	330	690	112
φ/(°)	38.76	36.40	39.07	37.80	31.53

3.5. Sample Destruction Images and Strain–Volumetric Deformation Curves at Different Temperatures and Optimal Mixing Ratios

Figures 6 and 7 show the improved aeolian sand strain–volumetric deformation curves and specimen failure images under the optimal mixing ratio and different temperature conditions, respectively.

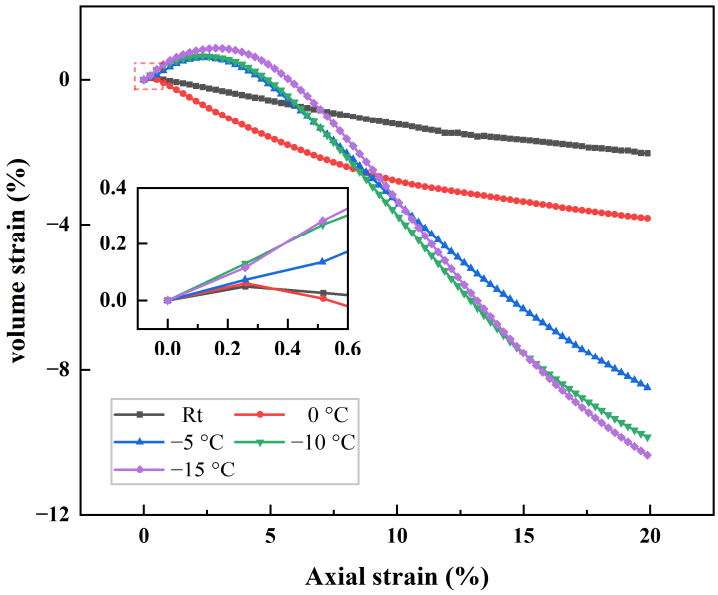

Figure 6. The modified aeolian sand strain–volumetric deformation curves under different temperature and the optimal blending conditions.

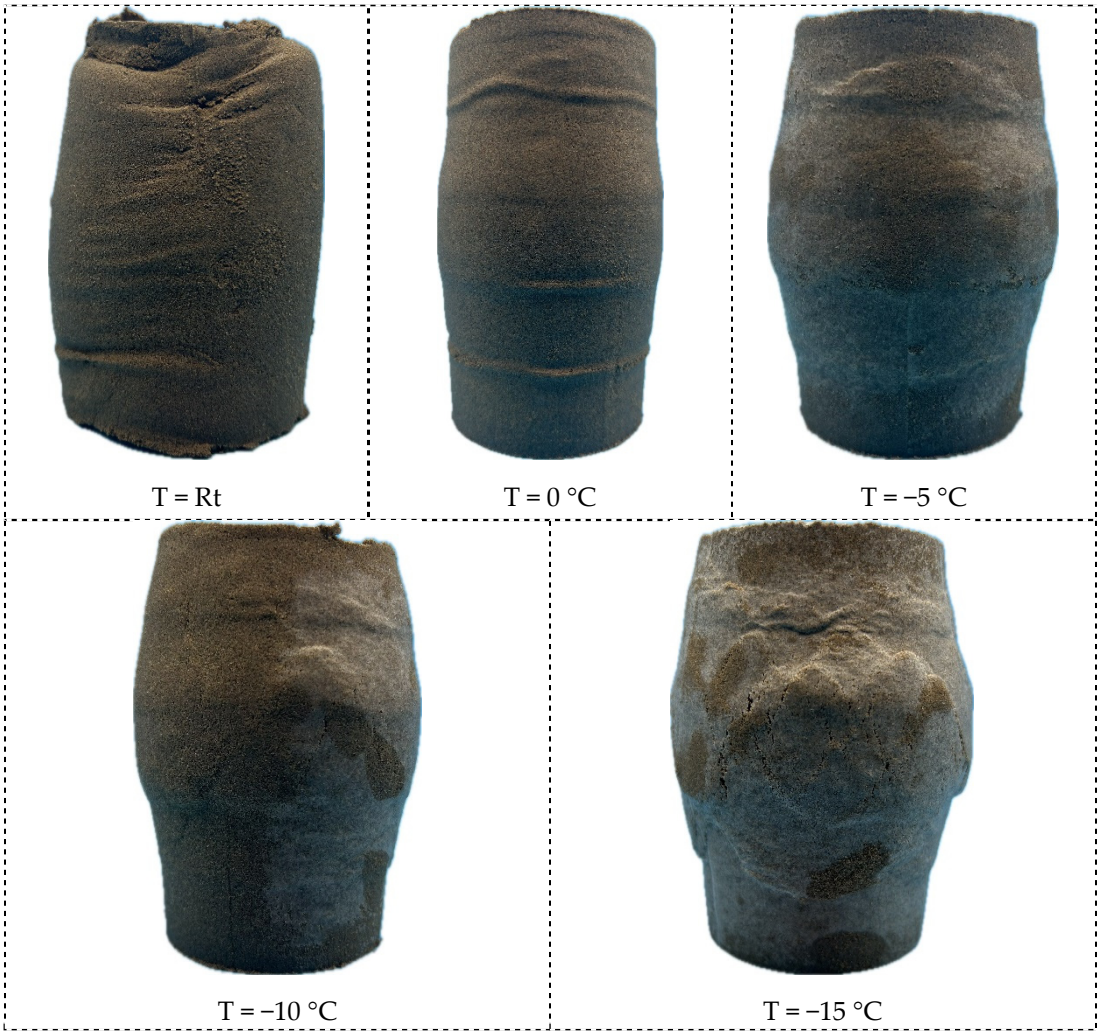

Figure 7. Test sample failure images.

It is not difficult to find from the combined stress–strain curve that there is an inseparable relationship among stress–strain–volumetric deformation curves. The samples exhibit the same properties at different temperatures: before reaching the peak strength, the specimen is in a shearing and shrinking state; after reaching the peak strength, the specimen transitions to a shearing and expanding state.

At room temperature and 0 °C, the shear contraction state transitions to a shear expansion state with a small strain, with both maximum shear contraction and maximum shear expansion being relatively small. From the damage diagram, it can be seen that oblique cracks appeared in the specimens at room temperature and 0 °C. As the temperature continues to decrease, the shear contraction to shear expansion transition point strain increases, and both the maximum volumetric contraction and maximum shear expansion increase significantly. After loading, the sample shows accumulation and expansion, and even fine cracks appear at −15 °C.

As depicted in Figure 7, when T = Rt, the sample suffered shear failure. Following the failure, the height significantly decreased without evident cracks or fragments falling off; when T = 0 °C, the sample underwent expansion failure, with the surface still maintaining its integrity. Only subtle texture changes could be observed, suggesting that a mild decrease in temperature had little impact on the mechanical properties of the sample; when T = −5 °C, the sample exhibited dilatancy failure, with more obvious layering marks apparent on its surface. This indicates that as the temperature decreases, the material's brittleness increases, thereby reducing its ability to resist external forces; T = −10 °C, the sample experienced shear dilatancy failure, with more prominent signs of damage. In some local areas on the surface, slight detachment or cracks may have already appeared; when T = −15 °C, the sample experienced shear dilatancy failure with a higher degree of surface damage, enabling the observation of more distinct detachment or cracks.

4. Discussion

This study analyzes the effects of different temperatures, various silt dosages, and confining pressure conditions on the mechanical properties of silt-modified aeolian sand through a series of temperature-controlled triaxial compression tests. (1) By introducing temperature-controlled conditions, the study systematically analyzes the impact of temperature changes on the mechanical properties of silt-modified aeolian sand. The research results not only focus on the improvement of the strength of the modified aeolian sand but also explore its adaptability under different environmental and stress conditions. (2) By combining three major factors: temperature, silt dosage, and confining pressure conditions, the study reveals their synergistic effects on the mechanical properties of modified aeolian sand through multi-parameter system analysis. (3) The optimal silt dosage was obtained through experiments, which can not only enhance the modification effect but can also reduce modification costs, achieving a balance between economy and performance.

As mentioned earlier, the addition of silt, changes in confining pressures, and temperature variations all affect the stress–strain curve of aeolian sand. The results of this study indicate that:

(1) The stress–strain behavior of the samples under different confining pressures tests tends to be consistent, showing that as the strain increases, the stress first increases to a peak value, then decreases and stabilizes. This change and trend are consistent with the results presented in [22].

(2) As the content of silt increases, the strength of triaxial compression shows a trend of first increasing and then decreasing. In similar studies, Radoslaw L. Michalowski and Michalowski, R.L. et al. found that with fiber-reinforced sand, the peak strength first increases and then decreases with the increase in fiber content [23]. This is consistent with the pattern observed in this study.

5. Conclusions

Through a series of indoor temperature control triaxial compression tests, an initial study was conducted on the mechanical properties of aeolian sand improved with silt. The primary findings can be summarized as follows:

(1) The optimal blending ratio for aeolian sand improved with silt is 15%. Compared with silt mixed with 0% aeolian sand, aeolian sand improved with silt exhibits significant improvement when silt is mixed at 15%. Under different silt dosage ratios, the improved aeolian sand stress–strain curves all exhibit strain softening. When aeolian sand improved with silt is mixed with 15% silt, its peak strength is significantly higher compared to other improved aeolian sand peak strengths under various dosages.

(2) Under optimal blending conditions (W_S = 15%), the strength characteristics of weathered sand and mud were compared under different stress constraints (σ_3 = 100, 200, 300 kPa) and temperatures (T = Rt, 0, −5, −10, −15 °C): when the temperature decreased from room temperature to 0 °C, there was a slight decrease in tensile strength and peak strength; as the temperature continued to drop, the tensile strength and peak strength showed significant increased; the greater the temperature, the more densely packed the overall stress path was under different stress constraint conditions.

(3) For aeolian sand improved with silt under varying temperature conditions, cohesion exhibits a trend of first increasing and then decreasing as the temperature decreases from room temperature to −15 °C; the friction angle remains fairly constant as the temperature decreases from room temperature to −10 °C, but significantly reduces at −15 °C.

(4) By examining the stress–strain curve and the volumetric deformation–strain curve together, it becomes evident that there exists an inextricable connection between stress, strain, and volumetric deformation. Upon attaining its peak strength, the sample undergoes volumetric expansion or contraction accompanying the body change.

This study only considers the behavior of materials in static or slow loading conditions with the triaxial test. Dynamic, cyclic, or complex stress state triaxial tests are needed to complement the shortcomings of the aeolian sand improved with silt experimental results. At the same time, the impact of aeolian sand from different regions on their mechanical properties still needs to be tested.

Author Contributions: Conceptualization, B.C. and X.S.; methodology, B.C. and X.S.; software, B.C.; validation, B.C., D.X. and B.Z.; formal analysis, B.C. and X.S.; investigation, J.X.; resources, J.X.; data curation, B.C.; writing—original draft preparation, B.C.; writing—review and editing, B.C. and X.S.; visualization, B.C.; supervision, J.X.; project administration, J.X.; funding acquisition, J.X. All authors have read and agreed to the published version of the manuscript.

Funding: This research was funded by the aeolian sand Embankment Technology and Mechanical Performance Research Enterprise-School Collaboration Project Fund (GDXZ20200618) and Gansu Agricultural University's Funding for Discipline Construction in 2024 (Water Resources Engineering Discipline Construction) Fee for Building Disciplinary Teams (27000102).

Data Availability Statement: The data used in this study are confidential.

Acknowledgments: We would like to express my sincerest gratitude to Jian Xu for his guidance.

Conflicts of Interest: The authors declare no conflicts of interest.

Abbreviations

W_S	Silt concentrations
σ_3	Confining pressures
K	Consolidation ratio
γ	Shearing speed

T	Temperature
Rt	Room temperature (20 °C)
ω_0	Optimal water content
ρ_{dmax}	Maximum density
c	Cohesion
φ	Friction angle
p	Maximum effective principal stress
q	Minimum effective principal stress

References

1. Zhang, H.; Wang, Z.; Liu, R.; Li, L. Study of Static Mechanical Properties of Aeolian Sand. *Appl. Mech. Mater.* **2014**, *587–589*, 976–980. [CrossRef]
2. Chen, Y. Research on the Engineering Properties of aeolian sand and Its Application in the Management of Goaf Areas. *Energy Technol. Manag.* **2023**, *481*, 74–77.
3. Zhao, Y.; Zhao, Y.; Han, J. Aeolian sand Engineering Characteristics Test Research. *Heilongjiang Sci. Technol. Inf.* **2009**, *13*, 56.
4. Zheng, M.; Wang, Q.; Chen, W.; Gao, Y.; Zhang, S.; Zhun, L. Material properties and shear strength of aeolian sand in different regions. *Chin. Sci. Pap.* **2021**, *16*, 415–421.
5. Huang, C.; Yuan, Z.; Yang, B. Analysis of Influencing Factors on Unconfined Compressive Strength of aeolian sand Cement Amendments. *Constr. Build. Mater.* **2023**, *20*, 2858–2867.
6. Yang, X.; Hu, Z.; Wang, Y.; Wang, X. Aeolian sand stabilized by using fiber- and silt-reinforced cement: Mechanical properties, microstructure evolution, and reinforcement mechanism. *China Highw. J.* **2024**, *411*, 134750. [CrossRef]
7. Ruan, B.; Zhao, Y.; Zhang, X.; Yuan, Z.; Che, Y.; Lu, Z. Study on the Strength and Microstructure of Short Fiber-Reinforced Cement with Different Lengths for aeolian sand. *Railw. Sci. Eng. J.* **2024**, *46*, 1–11.
8. Ruan, B.; Shen, Y.; Zhang, X.; Lu, Z.; Zhang, J.; Nie, R. Research on the Dynamic Properties of Fiber Cement under Freezing-Thawing Cycles. *Railw. Sci. Eng. J.* **2024**, *46*, 1–9.
9. Wei, J.; Zhao, Y.; Yang, Y. A Study on the Gradation Characteristics of aeolian sand Blended Sand Mixtures. *Low Temp. Build. Technol.* **2016**, *10*, 112–114+133.
10. Jing, P.; Zhang, Y.; Song, X.; Zhang, L.; Yang, H.; Yu, T.; Wang, P. Study on the Impact of Intense Rainfall and High Temperature Weather on the Hydrodynamic Characteristics of aeolian sand Roadbed. *Railw. Sci. Eng. J.* **2024**, *46*, 1–12.
11. Bao, W.; Li, W.; Mao, X.; Chen, R.; Qin, C.; Liu, Y. Soil Salinity under Freeze-Thaw Cycles: Mechanical Properties of aeolian sand Salt-Saturated Soils. *J. Transp. Eng.* **2023**, *23*, 114–124.
12. Liu, W.; Tian, Z.; Lu, Y.; Xu, J.; Gong, Z.; Wu, Y. Properties of aeolian sand and triaxial compression Blends with Cement silt. *Water Resour. Hydro-Power Sci. Technol. Prog.* **2023**, *43*, 51–57.
13. Gan, T.; Xu, J. Shimao Zhang Research on aeolian sand Dam Embankment Compaction Process Performance Test. *People's Yangtze River* **2023**, *54*, 140–146.
14. Pan, L.; Xu, J.; Gong, Z.; Zhang, S.; Tian, Z.; Gan, T. Study on compaction and shear characteristics of silt modified aeolian sand as dam filling material. *Water Resour. Hydropower Eng. (Chin. Engl.)* **2023**, *54*, 187–195.
15. Jia, W.; Kai, L.; Ding, X. Physical and mechanical properties of aeolian sand along the main stream of the Tarim River and its influencing mechanism. *J. Chongqing Univ.* **2024**, *65*, 1–10.
16. Bol, E.; Önalp, A.; Arel, E.; Sert, S.; Özocak, A. Liquefaction of silts: The Adapazari criteria. *Bull. Earthq. Eng.* **2010**, *8*, 859–873. [CrossRef]
17. Wang, L.; Ling, X.; Xu, X.; Gu, Q.; Hu, Q.L. Comparison of dynamic and static triaxial tests on frozen powdery clay along the Qinghai-Tibet Railway. *Chin. J. Geotech. Eng.* **2005**, *27*, 202–205.
18. *GB/T 50123-2019*; Standard for Geotechnical Testing Method. Chinese National Standard: Beijing, China, 2019.
19. Mao, Z.; Geng, M.; Bi, Y.; An, N. Time Effect Study on Purple-flowered Clover-Sand Composite shear strength. *Coal Sci. Technol.* **2023**, *11*, 234–247.
20. Huang, W.; Mao, X.; Wu, Q.; Chen, L. Experimental study on shear characteristics of the silty clay soil-ice interface. *Sci. Rep.* **2022**, *1*, 19687. [CrossRef]
21. Li, Z.; Sun, Y.; Jiang, X.; Jiang, J. A Study on the Mechanical Properties of Soil- stone Mixtures for Earth and Rock Dam Embankments under Various Temperatures Using Low confining pressures. *J. Hehai Univ. (Nat. Sci. Ed.)* **2024**, *52*, 90–96.
22. Li, Y.; Yang, S.-Q.; Liu, Z.-L.; Sun, B.-W.; Yang, J.; Xu, J. Study on mechanical properties and deformation of coal specimens under different confining pressure and strain rate. *Theor. Appl. Fract. Mech.* **2022**, *118*, 103287. [CrossRef]
23. Michalowski, R.L.; Čermák, J. Triaxial Compression of Sand Reinforced with Fibers. *J. Geotech. Geoenviron. Eng.* **2003**, *2*, 129. [CrossRef]